

Noncovalent Interactions between Unsolvated Peptides: Dissociation of Helical and Globular Peptide Complexes

David T. Kaleta and Martin F. Jarrold*

Department of Chemistry, Indiana University, 800 East Kirkwood Avenue, Bloomington, Indiana 47405

Received: January 9, 2003; In Final Form: June 18, 2003

The thermally activated unimolecular dissociation of some unsolvated complexes of helical and globular alanine/glycine-based peptides have been studied by electrospray mass spectrometry and ion mobility measurements. Rate constants have been measured as a function of temperature, and activation energies and entropies have been determined for dissociation of the $\text{Ac}-(\text{GA})_7\text{K}\cdot\text{Ac}-\text{A}(\text{GA})_7\text{K} + 2\text{H}^+$ (Ac = acetyl, G = glycine, A = alanine, and K = lysine) dimer (dominant conformation assigned to a V-shaped helical dimer) and the $2\text{Ac}-(\text{GA})_7\text{K}\cdot\text{Ac}-\text{A}(\text{GA})_7\text{K} + 3\text{H}^+$ and $\text{Ac}-(\text{GA})_7\text{K}\cdot 2\text{Ac}-\text{A}(\text{GA})_7\text{K} + 3\text{H}^+$ trimers (dominant conformation assigned to a pinwheel-shaped helical trimer). The activation energies were found to be 91 kJ mol^{-1} for the dissociation of the dimer, and 72 and 77 kJ mol^{-1} for dissociation of the trimers. A key advantage of the experimental approach described here is that it permits the conformations of the dissociating peptides to be observed. For the $\text{Ac}-\text{K}(\text{GA})_7\cdot\text{Ac}-\text{KA}(\text{GA})_7 + 2\text{H}^+$ dimer (which has the lysines at the N-terminus), there are two major conformations present (assigned to a compact globular aggregate and an antiparallel helical dimer) which appear to dissociate with different rates. The $\text{Ac}-\text{K}(\text{GA})_7\cdot\text{Ac}-\text{KA}(\text{GA})_7 + 2\text{H}^+$ dimers dissociate at a significantly higher temperature than the V-shaped $\text{Ac}-(\text{GA})_7\text{K}\cdot\text{Ac}-\text{A}(\text{GA})_7\text{K} + 2\text{H}^+$ dimer. The alanine analogue of the antiparallel helical dimer, $\text{Ac}-\text{KA}_{14}\cdot\text{Ac}-\text{KA}_{15} + 2\text{H}^+$, does not dissociate significantly at the highest temperature accessible ($\sim 423 \text{ K}$).

Introduction

Strong covalent bonds link amino acids into linear chains, but much weaker noncovalent interactions are responsible for the development of secondary structure, the assembly of tertiary structure domains, the formation of protein assemblies, and the regulatory interactions between proteins.¹ Understanding these noncovalent interactions is obviously crucial to deciphering the inner workings of biological activity. Studies investigating these interactions range from examining the interrelationships between protein hetero- and homodimers^{2,3} to the toxic activity of human pathogens⁴ and the action of HIV drugs.⁵ In addition to intramolecular and intermolecular noncovalent interactions within and between proteins, the interactions with the environment are also critically important. Separating the protein–protein and environmental contributions is difficult, but it is necessary to resolve these contributions in order to understand the interactions.⁶ Many studies have been performed in aqueous solution. However, there are other environments that are important. Membrane proteins, for example, comprise a significant class of proteins that operate in conditions vastly different from aqueous solution.^{7–10} One approach to separating environmental interactions from protein–protein interactions is to study unsolvated proteins and peptides in the gas phase.^{11,12}

In this article we describe studies of the dissociation of unsolvated dimers and trimers of helical and globular alanine/glycine-based peptides. We are studying these simple complexes as models for the development of tertiary structure domains within proteins and for the interactions between proteins. The complexes are produced by electrospray.¹³ Previous work has shown that electrospray can transfer weakly bound noncovalent complexes into the gas phase,^{14–16} and there have been several reports of the formation of peptide aggregates.^{17–19} We use ion

mobility mass spectrometry to investigate the complexes. The mobility of an ion in an inert buffer gas depends on the ion's average collision cross section, which, in turn, can be related to its structure.^{20–22} Ions with compact conformations undergo fewer collisions with the buffer gas and travel more rapidly than ions with more open conformations. Ion mobility measurements can easily distinguish between helical and globular conformations in unsolvated monomeric peptides²³ and have been used in several studies to examine the relative stabilities and properties of unsolvated helices.^{24–27} It is also possible to follow conformational changes that occur as the ions travel through the apparatus and to determine rate constants for these changes.²⁸ This approach has recently been used to examine the unfolding of an α -helix²⁹ and to study conformational changes in oligonucleotides.³⁰ A similar approach can be used to study thermally activated dissociation of peptides, proteins, and their complexes as they travel through the ion mobility apparatus. Bowers and co-workers have recently reported Arrhenius parameters for the dissociation of bradykinin and LHRH dimers.³¹ In related work, Williams and co-workers have used another mass spectrometry based technique, blackbody infrared radiative dissociation,^{32–34} to determine Arrhenius parameters for the dissociation of DNA dimers.³⁵ Klassen and co-workers have used the same approach to examine the dissociation of the SLT-1 pentamer³⁶ and to study the dissociation of the complexes between oligosaccharides and the Se155-4 antibody single chain fragment (scFv).³⁷

In a preceding paper, we reported studies of the conformations of the dimers and trimers generated by mixtures of helix-forming $\text{Ac}-(\text{GA})_7\text{K}$ & $\text{Ac}-\text{A}(\text{GA})_7\text{K}$ (Ac = acetyl, G = glycine, A = alanine, and K = lysine) peptides and globule-forming $\text{Ac}-\text{K}(\text{GA})_7$ & $\text{Ac}-\text{KA}(\text{GA})_7$ peptides.^{38,39} We used mixtures of slightly different peptides in these studies so that the complexes

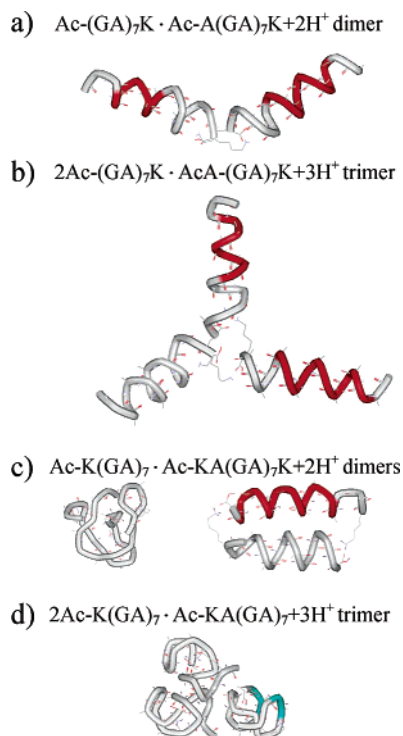


Figure 1. Conformations of the complexes studied here as determined by ion mobility measurements (for a complete discussion, see ref 39). Dominant conformations for the dimer (a) and trimer (b) from an $\text{Ac-(GA)}_7\text{K}$ & $\text{Ac-A(GA)}_7\text{K}$ mixture (helix-forming peptides) and the dimers (c) and trimer (d) generated from an Ac-K(GA)_7 & $\text{Ac-KA(GA)}_7\text{K}$ mixture (globule-forming peptides). The conformations originate from molecular dynamics simulations; they are low energy conformations that have calculated cross sections within 2% of the measured values (the normally accepted error margin in these studies). The images were produced using WebLab ViewerLite 3.5 (Molecular Simulations Inc., now Accelrys, San Diego, CA). The red regions are α -helix.

have a unique mass-to-charge ratio. The difference between the helix-forming and globule-forming peptides mentioned above is the location of the lysine: when the lysine is at the N-terminus the peptides are globular, and when the lysine is at the C-terminus the peptides are predominantly helical. The explanation for this behavior is that the electrosprayed peptides are protonated and the protonation site appears to be the lysine side chain. When the lysine is at the C-terminus, favorable interactions between the charge and the helix dipole promote helix formation while protonation near the N-terminus destabilizes the helix.^{19,23} Previous work has indicated that dimers from the mixture of helix-forming peptides ($\text{Ac-(GA)}_7\text{K}$ & $\text{Ac-A(GA)}_7\text{K}$) are predominantly V-shaped helical dimers, as shown in Figure 1a.³⁹ The conformations presented in Figure 1 originate from molecular dynamics simulations; they are low energy conformations that have calculated cross sections within 2% of the measured values (the normally accepted error margin in these studies).

Ion mobility measurements is one of the few methods that can provide useful structural information for these large complex systems in the gas phase. However, even with this approach, it is virtually impossible to deduce structural information about near-spherical conformations because there are so many candidate geometries that fit the measured cross section. However, the situation improves dramatically as the geometry distorts from spherical (and the cross section increases) because the number of low energy geometries that will fit the measured cross section decreases substantially. Thus for the $\text{Ac-(GA)}_7\text{K} \cdot \text{Ac-A(GA)}_7\text{K} + 2\text{H}^+$ complex mentioned above, the very elongated V-shaped

helical dimer geometry is really the only plausible low energy structure that will fit the measured cross section. A more detailed discussion of how the geometries are assigned to the complexes can be found in ref 39.

Trimers formed from the $\text{Ac-(GA)}_7\text{K}$ & $\text{Ac-A(GA)}_7\text{K}$ mixture appear to have primarily a pinwheel configuration, as shown in Figure 1b. The V-shaped dimer and pinwheel trimer conformations mentioned above have exchanged lysines: the protonated lysine of one peptide interacts with the C-terminus of the other peptide(s) in the complex. At first glance these conformations seem unfavorable because the charges are close together; however, there is a cooperative electrostatic stabilization whereby all the charges interact favorably with all the helix dipoles. The dimers produced from the mixtures of the globule-forming peptides (Ac-K(GA)_7 & $\text{Ac-KA(GA)}_7\text{K}$) which have the lysine at the N-terminus are either a compact globular aggregate or antiparallel helical dimers; both are shown in Figure 1c. In the antiparallel helical dimers the helices are in a head-to-toe arrangement where they can be stabilized by the exchanged lysines. The trimers produced from the Ac-K(GA)_7 & $\text{Ac-KA(GA)}_7\text{K}$ mixture appear to be primarily globular aggregates, as shown in Figure 1d.

In the studies reported here, the thermally activated unimolecular dissociation of these peptide aggregates is investigated by mass spectrometry and ion mobility measurements. In some cases, rate constants for dissociation were obtained as a function of temperature from which Arrhenius activation energies and preexponential factors were derived. A key advantage of the approach adopted here is that it is possible to examine the conformations of the dissociating peptides.

Materials and Methods

Peptide Synthesis. The peptides were synthesized using FastMoc chemistry with an Applied Biosystems Model 433A peptide synthesizer. After synthesis, the peptides were cleaved from the solid substrate with a 95% trifluoroacetic acid (TFA)/5% water solution, precipitated from solution with cold ethyl ether, washed, and lyophilized. Solutions of 1–2 mg of each peptide in 1 mL of 90% TFA/10% water were electrosprayed.

Instrumentation. The experimental apparatus has been described previously.²⁹ An electrospray source generates ions which enter a heated stainless steel capillary interface where they are desolvated. The capillary was maintained at a temperature of 110 °C. The desolvated ions are injected into the 30.5 cm long temperature-variable drift tube with an injection energy of 300 V. The helium buffer gas pressure was 2–5 Torr (depending on the temperature). Microprocessor-based temperature controllers maintain the temperature of the four drift tube sections to within <1 °C. The ions travel through the drift tube under the influence of a uniform electric field generated by drift voltages of 280–480 V. Ions that exit the drift tube are focused into a quadrupole mass spectrometer where they are mass selected and finally detected by an off-axis collision dynode and dual microchannel plates. Drift time distributions (the amount of time it takes for ions to travel across the drift tube) are determined using an electrostatic shutter to admit short (100 μs) pulses of ions into the drift tube and recording their arrival time distribution at the detector. The drift time distribution is then obtained by correcting the arrival time distribution for the time the ions spend traveling outside of the drift tube. The drift times can then be converted into collision cross sections using standard methods.⁴⁰

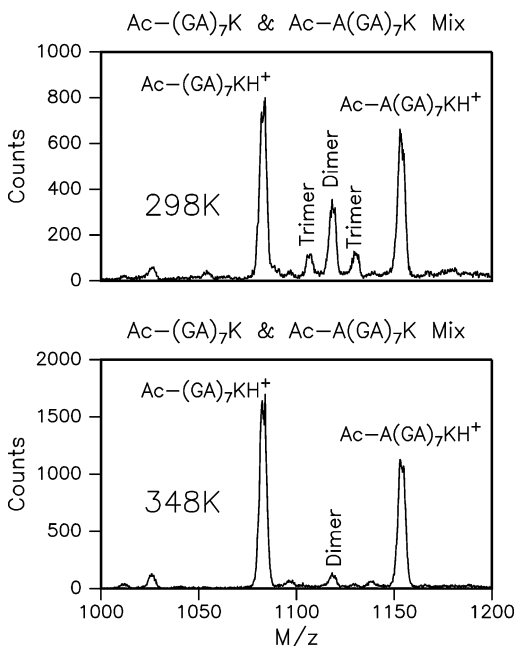


Figure 2. Electrospray mass spectra recorded for a 1:1 mixture of Ac-(GA)₇K & Ac-A(GA)₇K in 90% TFA/10% water with drift tube temperatures of 298 and 348 K. Peaks due to the Ac-(GA)₇K·Ac-A(GA)₇K + 2H⁺ dimer and the 2Ac-(GA)₇K·Ac-A(GA)₇K + 3H⁺ and Ac-(GA)₇K·2Ac-A(GA)₇K + 3H⁺ trimers are abundant at the lower temperature, but significantly diminished at the higher temperature.

Results

The Ac-(GA)₇K & Ac-A(GA)₇K Mixture. Figure 2 shows examples of mass spectra obtained by electrospraying a 1:1 mixture of Ac-(GA)₇K & Ac-A(GA)₇K at two drift tube temperatures: 298 and 348 K. Peaks for the Ac-(GA)₇K·Ac-A(GA)₇K + 2H⁺ dimer and the 2Ac-(GA)₇K·Ac-A(GA)₇K + 3H⁺ and Ac-(GA)₇K·2Ac-A(GA)₇K + 3H⁺ trimers are clearly evident between the monomer peaks at the lower temperature. The relative abundance of the multimers diminishes at the higher temperature (see Figure 2). In previous work, the dimer was found to be predominantly in the V-shaped arrangement shown in Figure 1a, while the trimers were found to be mainly in the pinwheel configuration shown in Figure 1b.

When the trimer and dimer ions dissociate, we expect that two ions will be produced (a dimer ion and a monomer ion from a trimer ion and two monomer ions from a dimer ion). Thus, the total number of ions in the mass spectrum is expected to change as the multimers dissociate. To account for this, we define a conserved intensity (which does not change as the multimers dissociate):

$$I_{\text{CON}} = I_{\text{LM}} + I_{\text{HM}} + 3I_{\text{D}} + \frac{11(I_{\text{HT}} + I_{\text{LT}})}{3} \quad (1)$$

In this expression we have accounted for hidden dimers and trimers at the same nominal mass as the monomers by assuming that they have the same relative abundance as the mixed dimers and trimers. I_{LM} , I_{HM} , I_{D} , I_{HT} , and I_{LT} are the relative intensities from the mass spectra of the low (mass) monomer, high monomer, mixed dimer, low trimer, and high trimer, respectively. The corrected relative abundances of the dimer, low trimer, and high trimer are then given by

$$\text{RA}_{\text{D}} = \frac{2I_{\text{D}}}{I_{\text{CON}}}; \quad \text{RA}_{\text{LT}} = \frac{3I_{\text{LT}}}{I_{\text{CON}}}; \quad \text{RA}_{\text{HT}} = \frac{3I_{\text{HT}}}{I_{\text{CON}}} \quad (2)$$

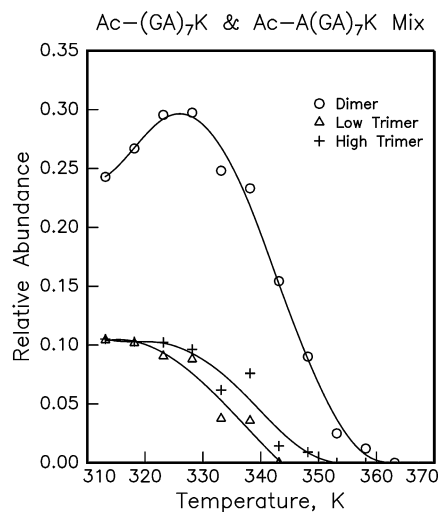


Figure 3. Plot of corrected relative abundances (see text) of Ac-(GA)₇K·Ac-A(GA)₇K + 2H⁺ dimer (○) and 2Ac-(GA)₇K·Ac-A(GA)₇K + 3H⁺ (△) and Ac-(GA)₇K·2Ac-A(GA)₇K + 3H⁺ (+) trimers against drift tube temperature.

Figure 3 shows a plot of the corrected relative abundances of the Ac-(GA)₇K·Ac-A(GA)₇K + 2H⁺ dimer and the 2Ac-(GA)₇K·Ac-A(GA)₇K + 3H⁺ and Ac-(GA)₇K·2Ac-A(GA)₇K + 3H⁺ trimers as a function of drift tube temperature. The relative abundance of dimer initially increases slightly and then smoothly decreases and ultimately vanishes as the temperature is raised further and the dimer dissociates. The trimers also disappear as the temperature is raised. The results for the two trimers are almost identical. The trimers appear to dissociate at a slightly lower temperature than the dimer.

Figure 4 shows the drift time distributions for the Ac-(GA)₇K·Ac-A(GA)₇K + 2H⁺ dimer recorded with drift tube temperatures of 298, 323, 338, and 348 K. At room temperature (298 K) three peaks are evident, indicating three structures with different cross sections. The most abundant peak, which also has the longest drift time (largest cross section), has been assigned to the V-shaped helical dimer shown in Figure 1a. The middle peak has been assigned to a parallel helical dimer with one helix offset from the other, and the peak with the shortest drift time (smallest cross section) has been assigned to a globular aggregate.³⁹ Upon raising the temperature to just below the point where dissociation begins (323 K), it is evident that the middle peak and the peak with the shortest drift time have diminished significantly. There remains a small peak at short drift time which stays relatively constant as the temperature is raised further and the dimer dissociates. From these results we can conclude that in the temperature range where dissociation occurs the dominant feature present is the one assigned to the V-shaped helical dimer shown in Figure 1a. At the highest temperature in Figure 4 a poorly resolved shoulder appears on the short time side of the dominant peak. This may represent another conformation or a variation of the V-shaped helical dimer geometry.

To determine rate constants for the dissociation of the Ac-(GA)₇K·Ac-A(GA)₇K + 2H⁺ dimer, mass spectra were recorded with drift voltages of 280, 380, and 480 V for drift tube temperatures between 328 and 353 K. Changing the drift voltages changes the amount of time that the ions spend traveling through the drift tube (the reaction time). Figure 5 shows the natural logarithm of the corrected dimer relative abundances plotted against the average time spent in the drift tube (from the measured drift time distributions). Ideally, the slopes of these plots are the rate constants for dissociation at each temperature. However, in the present case, the values derived in this way

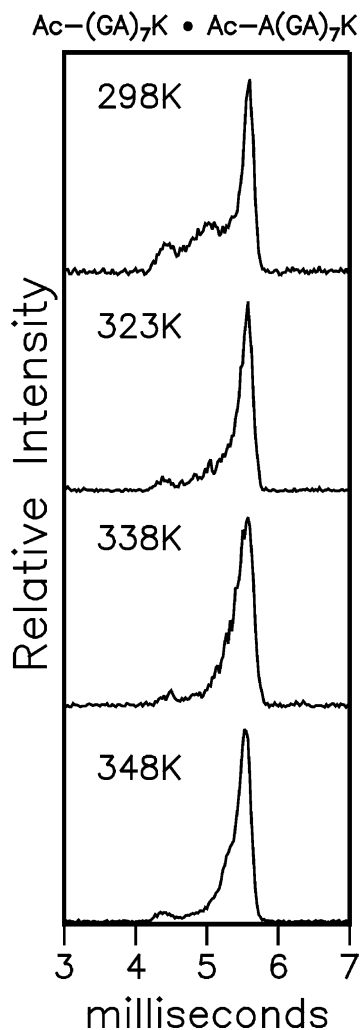
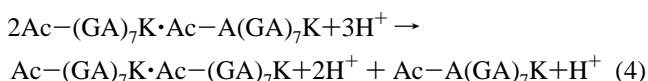
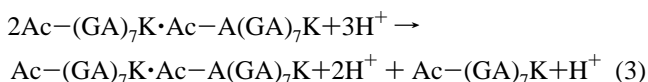


Figure 4. Drift time distributions recorded for $\text{Ac}-(\text{GA})_7\text{K}\cdot\text{Ac}-\text{A}(\text{GA})_7\text{K} + 2\text{H}^+$ dimer at drift tube temperatures of 298, 323, 338, and 348 K.

need to be corrected to account for the fact that the trimers are dissociating and contributing to the population of dimer at the same time as the dimer is dissociating. The trimers can presumably dissociate into either a homo- or heterodimer:



of which only the heterodimer is of interest. We assume that half the trimer populations contribute to the heterodimer. The trimer dissociates along the length of the drift tube, and this reduces the time available for dissociation for the dimer produced from the trimer. At high temperature the trimer dissociates near the entrance of the drift tube, while at low temperature the dimer is produced along the length of the drift tube. We could not devise a simple analytical correction to account for this behavior, so corrected rate constants were obtained by fitting a numerical simulation (which incorporates the trimer dissociation into dimers) to the kinetic data shown in Figure 5. The lines in Figure 5 show the resulting fits. The principal quantities required for the simulations are the rate constants for dissociation of the trimers and their initial relative

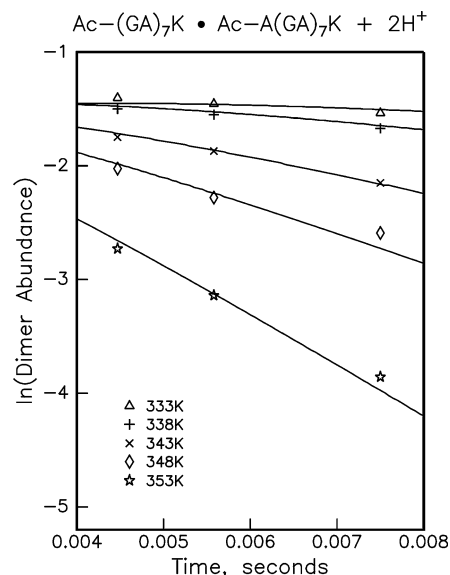


Figure 5. Plot of logarithm of corrected relative abundance of $\text{Ac}-(\text{GA})_7\text{K}\cdot\text{Ac}-\text{A}(\text{GA})_7\text{K} + 2\text{H}^+$ dimer against reaction time from measurements performed with different drift voltages (280, 380, and 480 V). The points are the measurements and the line is a least-squares fit of a numerical simulation to determine the corrected rate constants. The correction is for trimer dissociation (see text). Results are shown for a range of drift tube temperatures from 333 to 353 K.

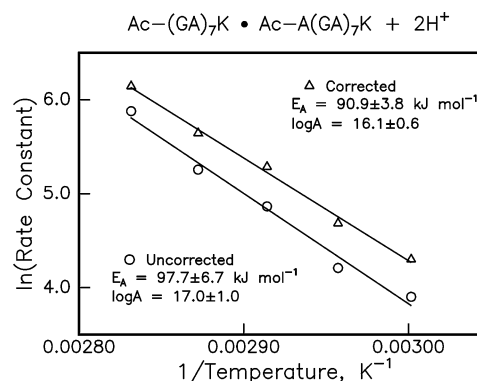


Figure 6. Arrhenius plot of logarithm of corrected and uncorrected rate constant for dissociation of $\text{Ac}-(\text{GA})_7\text{K}\cdot\text{Ac}-\text{A}(\text{GA})_7\text{K} + 2\text{H}^+$ dimer against $1/T$. The correction is for trimer dissociation (see text).

abundances. As described below, the rate constants for trimer dissociation can be derived directly from the data (because there are no tetramers present).

Figure 6 shows an Arrhenius plot of the natural logarithm of the uncorrected and corrected rate constants against $1/T$. The slope of this plot is the Arrhenius activation energy, E_a , and the intercept is the preexponential factor, A . The correction increases the rate constants by up to 60%. From the corrected rate constants we obtain $E_a = 90.9 \pm 3.8 \text{ kJ mol}^{-1}$ and the logarithm of the preexponential factor $\log A = 16.1 \pm 0.4$. From the uncorrected rate constants we obtain $E_a = 97.7 \pm 6.7 \text{ kJ mol}^{-1}$ and $\log A = 17.0 \pm 1.0$. Thus, at least in the present case, the correction does not make a large difference to the Arrhenius parameters.

The analysis of the results for the trimers parallels that described above for the dimer except that it is not necessary to correct for dissociation of higher complexes (the tetramer was not observed). The drift time distributions (DTDs) for the trimers are similar in appearance to that for the dimer, with three peaks at room temperature, though for the trimers the middle peak is more abundant than that for the dimer. The largest peak, which

TABLE 1: Arrhenius Activation Energy, E_a , Logarithm of the Preexponential Factor, $\log A$, and Activation Entropy, ΔS^\ddagger , for Dissociation of Dimers and Trimers from Ac-(GA)₇K & Ac-A(GA)₇K Mixture

peptide complex	E_a , kJ mol ⁻¹	$\log A$	ΔS^\ddagger , ^a J K ⁻¹ mol ⁻¹
Ac-(GA) ₇ K·Ac-A(GA) ₇ K + 2H ⁺ dimer (V-shaped)	90.9 ± 3.8	16.1 ± 0.6	54 ± 12
2Ac-(GA) ₇ K·Ac-A(GA) ₇ K + 3H ⁺ low trimer	72.4 ± 9.6	13.7 ± 1.5	8 ± 29
Ac-(GA) ₇ K·2Ac-A(GA) ₇ K + 3H ⁺ high trimer	77.2 ± 2.2	14.3 ± 0.3	19 ± 6

^a Entropy of activation at the middle of the experimental temperature range (338 K).

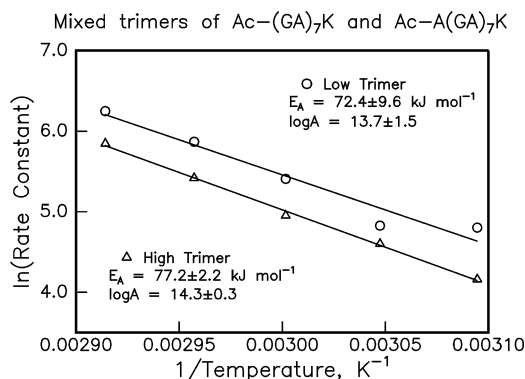


Figure 7. Arrhenius plot of logarithm of rate constant against $1/T$ for dissociation of low trimer ($2\text{Ac}-(\text{GA})_7\text{K}\cdot\text{Ac}-\text{A}(\text{GA})_7\text{K} + 3\text{H}^+$) and high trimer ($\text{Ac}-(\text{GA})_7\text{K}\cdot 2\text{Ac}-\text{A}(\text{GA})_7\text{K} + 3\text{H}^+$).

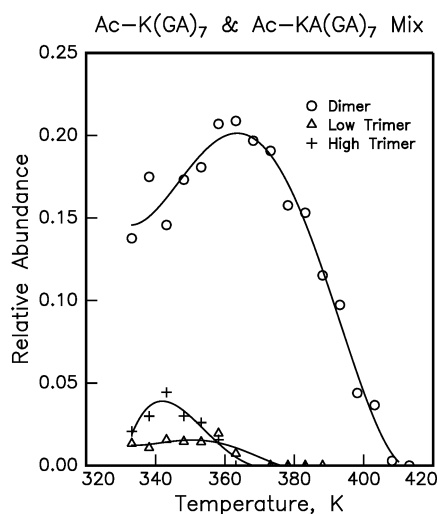


Figure 8. Plot of corrected relative abundances (see text) of Ac-K(GA)₇·Ac-KA(GA)₇ + 2H⁺ dimer (○) and 2Ac-K(GA)₇·Ac-KA(GA)₇ + 3H⁺ (Δ) and Ac-K(GA)₇·2Ac-KA(GA)₇ + 3H⁺ (+) trimers against drift tube temperature.

also had the largest cross section, was assigned to the pinwheel configuration shown in Figure 1b. The middle peak was assigned to a V-shaped dimer with an additional helix oriented antiparallel to one arm of the V. For the feature with the smallest cross section (the lowest abundance peak) a configuration with one helix and two globules was considered likely. As the temperature is raised to the point where dissociation begins, the middle peak essentially disappears, as with the dimer, and then the DTD remains virtually unchanged as the temperature is raised further. The dominant conformation present throughout the temperature range where dissociation occurs is the feature assigned to the pinwheel geometry shown in Figure 1b. Rate constants were derived by changing the drift voltage and plotting the relative abundance of the trimers against reaction time, as described for the dimer above. The Arrhenius plots for the trimers are shown in Figure 7, and the parameters derived from these plots are summarized in Table 1. For the low trimer, $2\text{Ac}-(\text{GA})_7\text{K}\cdot\text{Ac}-\text{A}(\text{GA})_7\text{K} + 3\text{H}^+$, we obtained $E_a = 72.4 \pm 9.6$ kJ mol⁻¹ and

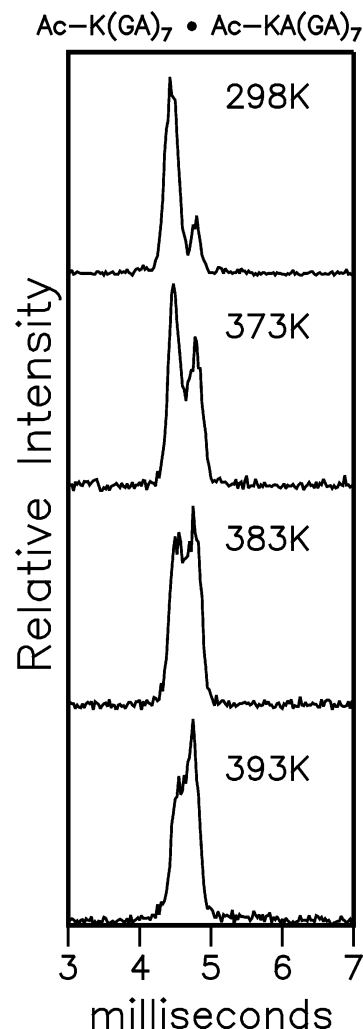


Figure 9. Drift time distributions recorded for Ac-K(GA)₇·Ac-KA(GA)₇ + 2H⁺ dimer at drift tube temperatures of 298, 373, 383, and 393 K.

$\log A = 13.7 \pm 1.5$; for the high trimer, $\text{Ac}-(\text{GA})_7\text{K} \cdot 2\text{Ac}-\text{A}(\text{GA})_7\text{K} + 3\text{H}^+$, we obtained $E_a = 77.2 \pm 2.2$ kJ mol⁻¹ and $\log A = 14.3 \pm 0.3$. Thus, the Arrhenius parameters derived for the dissociation of the two trimers are quite similar.

The Ac-K(GA)₇ & Ac-KA(GA)₇ Mixture. This mixture has a significantly lower abundance of multimers compared with the peptides with the lysines at the C-termini: the trimer abundances, in particular, are much smaller. Figure 8 shows the plot of the corrected relative abundances of the dimers and trimers over a drift tube temperature range of 333–408 K. The Ac-K(GA)₇·Ac-KA(GA)₇ + 2H⁺ dimer dissociates at a significantly higher temperature than the Ac-(GA)₇K·Ac-A(GA)₇K + 2H⁺ dimer discussed above. The trimers from the Ac-K(GA)₇ & Ac-KA(GA)₇ mixture also appear to dissociate at a higher temperature than the trimers from the Ac-(GA)₇K & Ac-A(GA)₇K mixture.

Figure 9 shows drift time distributions (DTD) recorded for the Ac-K(GA)₇·Ac-KA(GA)₇ + 2H⁺ dimer at several drift tube

temperatures. The two peaks present at room temperature have been assigned to a globular aggregate (the peak with the shorter drift time) and an antiparallel helical dimer.³⁹ Both these conformations are shown in Figure 1c. At room temperature the peak at shorter drift time is dominant, but as the temperature is raised the peak at longer drift times becomes the larger of the two. Thus it appears that either the globular aggregate is dissociating faster than the antiparallel helical dimer, or the globular aggregate is converting into the antiparallel helical dimer (or both). If one of the conformations is converting into the other, the peaks are expected to become less well resolved as the temperature is raised. This is observed in Figure 9. The dissociation of the Ac-K(GA)₇·Ac-KA(GA)₇ + 2H⁺ dimer is clearly a complex process involving at least two conformations which appear to interconvert and possibly dissociate at different rates. Under these circumstances the Arrhenius parameters for the overall dissociation process are not particularly useful quantities. The low abundance of trimers from the Ac-K(GA)₇ & Ac-KA(GA)₇ mixture precluded a more detailed study of their dissociation processes.

Ac-KA₁₄ & Ac-KA₁₅ and Ac-A₁₄K & Ac-A₁₅K Mixtures. The Ac-KA₁₄ & Ac-KA₁₅ mixture has a larger dimer relative abundance than the Ac-(GA)₇K & Ac-A(GA)₇K mixture, though trimers were not observed from the alanine peptides. The drift time distribution for the Ac-KA₁₄·Ac-KA₁₅ + 2H⁺ dimer contains a single peak, which was assigned to an antiparallel helical dimer similar to that shown in Figure 1c for Ac-K(GA)₇·Ac-KA(GA)₇ + 2H⁺. However, the Ac-KA₁₄·Ac-KA₁₅ + 2H⁺ antiparallel helical dimer does not dissociate significantly within the ~5–10 ms experimental time scale at the highest temperatures that can be accessed with the current apparatus (423 K). The Ac-A₁₄K & Ac-A₁₅K mixture has a low abundance of both dimers and trimers and was not investigated further.

Discussion

The Arrhenius preexponential factor can be related to the entropy of activation using transition state theory:^{41,42}

$$A = (ekT_m/h) \exp(\Delta S^\ddagger/R) \quad (5)$$

where k is Boltzmann's constant, T_m is the average temperature at which the measurements were made, h is Planck's constant, ΔS^\ddagger is the activation entropy, and R is the gas constant. Values for the entropy of activation obtained from the A factors are included in Table 1. The activation entropies are within the range expected for unimolecular dissociation of these complexes. Much larger A factors have been obtained using the FTMS-based method of blackbody infrared radiative dissociation, albeit for the dissociation of larger complexes.^{36,37}

Ac-(GA)₇K & Ac-A(GA)₇K Mixture. At room temperature the drift time distributions for the Ac-(GA)₇K·Ac-A(GA)₇K + 2H⁺ dimer show three features. As the temperature is raised to the point where the dimer starts to dissociate, the two features with short drift times diminish in intensity. However, as the temperature is raised further, and the dimer dissociates, the drift time distributions do not change significantly. The fact that the remaining features do not coalesce into a single peak as the temperature is raised indicates that the conformations that remain are not interconverting on the time scale of the experiment. Thus dissociation is occurring from several different conformations (though one is clearly dominant). Since the drift time distribution does not change significantly over the temperature range where dissociation is occurring, the different conformations must dissociate with very similar rates. If they did not all dissociate

with similar rates, the conformation that dissociates the slowest would be enriched as the temperature is raised or the reaction time increased.

The changes in the drift time distributions that occur below the temperature where dissociation starts must be the result of conformational changes. It seems that some of the population that contributes to the two features at short drift time must convert into the dominant feature at long drift time (the V-shaped helical dimer) as the temperature is raised above ambient. However, the fact that only some of the population at short drift time converts suggests that there are multiple conformations present (at least one that converts at low temperature and at least one that dissociates at higher temperature).

The dominant conformation present in the drift time distributions throughout the temperature range where the dimer dissociates has been assigned to the V-shaped helical dimer shown in Figure 1a. In this conformation the helices are held together by exchanged lysines. In the monomeric peptide the helical conformation is stabilized by the protonated lysine side chain capping the C-terminus. This stabilizes the helix through favorable interactions between the charge and the helix dipole and by providing hydrogen bonding partners for the dangling carbonyl groups at the C-terminus. In the V-shaped helical dimer, the lysine from one peptide caps the C-terminus of the other. This arrangement is stabilized by a cooperative electrostatic interaction where both charges interact favorably with the helix dipoles from both peptides. The V-shaped arrangement also minimizes unfavorable interactions between the helix dipoles. However, Coulomb repulsion between the localized charges destabilizes this arrangement, and overall, the V-shaped helical dimer is expected to be weakly bound relative to dissociation to two helical monomers.³⁹ On the other hand, separation of the helices requires that the lysines uncouple and exchange, and there is probably a significant activation barrier associated with this process. The measured activation energy is thus made up of the binding energy of the helical dimer relative to separated helical monomers plus the activation barrier for uncoupling the exchanged lysines. Probably the bulk of the measured activation energy of 90.9 ± 3.8 kJ mol⁻¹ is due to the activation barrier for uncoupling the lysines. The entropy of activation for dissociation of the dimer (derived from the Arrhenius preexponential factor) is relatively small, $\Delta S^\ddagger = 54$ J K⁻¹ mol⁻¹, indicating a fairly tight transition state. Such an organized transition state might be anticipated for a synchronized uncoupling of the two lysines.

The activation energies and entropies for the dissociation of the trimers are similar and smaller than for dissociation of the dimer ($E_a = 72.4 \pm 9.6$ and 77.2 ± 2.2 kJ mol⁻¹ versus 90.9 ± 3.8 kJ mol⁻¹; $\Delta S^\ddagger = 8 \pm 29$ and 19 ± 6 J K⁻¹ mol⁻¹ versus 54 ± 12 J K⁻¹ mol⁻¹). The similarity is expected because the trimers are closely related. The dominant feature present for the trimers was assigned to the pinwheel-shaped conformation shown in Figure 1b. This arrangement also has exchanged lysines with the helices arranged to minimize unfavorable interactions between their helix dipoles. For dissociation to occur it is necessary to uncouple and rearrange two of the exchanged lysines (as it is for dissociation of the V-shaped dimer). The slightly lower activation energy for the trimers may result because of the increased Coulomb repulsion in the trimer compared with the dimer. In the dimer there are two charges close together, while in the trimer there are three.

Viewing the helical components of the dimer and trimers as dipoles, the V-shaped arrangement of the dimer and the

pinwheel-shaped arrangement of the trimer result because aligned dipoles repel each other. Two dipoles pinned together (as in the dimer) have more flexibility than three. Thus, the dimer is expected to be more floppy than the trimer. The smaller entropy of activation for the dissociation of the trimers indicates a tighter (more restrictive) transition state. The fact that the trimers have more rigid geometries than the dimer may contribute to the smaller entropies of activation for the trimers.

Ac-K(GA)₇ & Ac-KA(GA)₇ Mixture. Unlike the Ac-(GA)₇K•Ac-A(GA)₇K + 2H⁺ dimer discussed above where there is a single dominant conformation (the V-shaped dimer), for the Ac-K(GA)₇•Ac-KA(GA)₇ + 2H⁺ dimer there are two major conformations: a globular aggregate and an antiparallel helical dimer. The helices in the antiparallel helical dimer are stabilized by the exchanged lysines. This stabilization is not possible for the monomers, so the preferred conformation of the monomers is a globule. Thus when the antiparallel helical dimer dissociates, a major conformational rearrangement must occur: from two helices in an antiparallel arrangement to two globules.

As the temperature is raised above ambient, the relative abundance of the helical dimer increases. Some of this increase happens below the temperature where dissociation starts to occur, so this must result from the conversion of some of the globular aggregate into the antiparallel helical dimer. The fact that only some of the globular aggregate converts is an indication that there are multiple forms of the globular aggregate, since the globular aggregate is not expected to have a well-defined structure; this is not unexpected. The enrichment in the antiparallel helical dimer above the temperature where dissociation starts to occur could result from either preferential dissociation of the globular aggregate or further conversion of the globular aggregate into helical dimer. The fact that the two peaks become poorly defined in the drift time distributions (see Figure 9) suggests that the latter is occurring, but does not rule out the former.

Despite the complex isomerization and dissociation processes that occur for the Ac-K(GA)₇•Ac-KA(GA)₇ + 2H⁺ dimer, it dissociates over a relatively narrow temperature range. Furthermore, the temperature where the Ac-K(GA)₇•Ac-KA(GA)₇ + 2H⁺ dimer dissociates is significantly higher than that for the V-shaped Ac-(GA)₇K•Ac-A(GA)₇K + 2H⁺ dimer. For the antiparallel helical dimer the higher dissociation temperature may simply result from the increased dissociation energy relative to that of the V-shaped Ac-(GA)₇K•Ac-A(GA)₇K + 2H⁺ dimer. The dissociation energy (the difference between the energy of the dimer and the energy of two separated monomers) of the V-shaped Ac-(GA)₇K•Ac-A(GA)₇K + 2H⁺ dimer is expected to be small because it is really only held together by the exchanged lysines. The Ac-K(GA)₇•Ac-KA(GA)₇ + 2H⁺ antiparallel helical dimer, on the other hand, is expected to have a larger dissociation energy because, in addition to the exchanged lysines, this dimer is bound by favorable interactions between the helix dipoles and by the fact that the helices must convert into globules when the dimer dissociates. The Ac-KA₁₄•Ac-KA₁₅ + 2H⁺ dimer does not dissociate over the accessible temperature range (up to 423 K) presumably because the presence of the additional alanine residues further stabilizes the helical conformation, making the energetic penalty for conversion from helix to globule larger, which increases the dissociation energy of the antiparallel helical dimer even further.

The higher dissociation temperature of the Ac-K(GA)₇•Ac-KA(GA)₇ + 2H⁺ globular aggregate relative to the Ac-(GA)₇K•Ac-A(GA)₇K + 2H⁺ V-shaped dimer also suggests a higher

dissociation energy for the former. We cannot distinguish from the drift time measurements whether the globular aggregate exists as two quite distinct self-solvated globules loosely bound together or as two entangled chains with each peptide interacting with the charge on both peptides. The significant dissociation energy implied by the results presented here is consistent with the entangled conformation. The close intimate interactions between the two chains in this arrangement would be expected to lead to a significant dissociation energy. The arrangement mentioned above with two loosely coupled globules may also exist, but it may convert into the antiparallel helical dimer as the temperature is raised.

Conclusions

Electrospray mass spectrometry and ion mobility measurements have been used to study the thermally activated unimolecular dissociation of some unsolvated complexes of helical and globular alanine/glycine-based peptides. Activation energies and entropies have been determined from rate constants measured as a function of temperature. The Ac-(GA)₇K•Ac-A(GA)₇K + 2H⁺ V-shaped helical dimer and the 2Ac-(GA)₇K•Ac-A(GA)₇K + 3H⁺ and Ac-(GA)₇K•2Ac-A(GA)₇K + 3H⁺ pinwheel-shaped helical trimers are believed to consist of helices pinned together by an exchanged lysine binding motif, where the lysine from one peptide interacts with the C-terminus of another. The activation energies measured for the dissociation of these complexes (91 kJ mol⁻¹ for the dissociation of the dimer, and 72 and 77 kJ mol⁻¹ for dissociation of the trimers) are thought to be largely due to the energy required to uncouple and reorganize the lysines. The smaller activation energies for the trimers is attributed to the higher charge on the larger complexes. The charge is localized at the junction between the helical peptides, and the buildup of charge probably also accounts for the absence of higher order complexes such as the tetramer and pentamer.

A key advantage of the experimental approach described here is that it permits the conformations of the dissociating peptides to be observed. For the Ac-K(GA)₇•Ac-KA(GA)₇ + 2H⁺ dimer (which has the lysines at the N-terminus), there are two major conformations present (a compact globular aggregate and an antiparallel helical dimer) which appear to dissociate with different rates. Dissociation of the Ac-K(GA)₇•Ac-KA(GA)₇ + 2H⁺ antiparallel helical dimer requires uncoupling of the lysine binding motifs and disruption of the helical domains (because the uncomplexed peptides have globular conformations, not helical). This explains why the Ac-K(GA)₇•Ac-KA(GA)₇ + 2H⁺ antiparallel helical dimers dissociate at a significantly higher temperature than the V-shaped Ac-(GA)₇K•Ac-A(GA)₇K + 2H⁺ helical dimer.

Acknowledgment. We thank Jiri Kolafa for the use of his MACSIMUS molecular modeling programs. We gratefully acknowledge the support of this work by the National Institutes of Health.

References and Notes

- (1) Branden, C.; Tooze, J. *Introduction to Protein Structure*, 2nd ed.; Garland: New York, 1999.
- (2) Doyle, S. M.; Braswell, E. H.; Teschke, C. M. *Biochemistry* **2000**, *39*, 11667–11676.
- (3) Kim, D. H.; Nam, G. H.; Jang, D. S.; Yun, S.; Choi, G.; Lee, H. C.; Choi, K. Y. *Protein Sci.* **2001**, *10*, 741–752.
- (4) Fivaz, M.; Velluz, M. C.; van der Goot, F. G. *J. Biol. Chem.* **1999**, *274*, 37705–37708.
- (5) Sluis-Cremer, N.; Arion, D.; Parniak, M. A. *Mol. Pharmacol.* **2002**, *62*, 398–405.

- (6) Dill, K. A. *Biochemistry* **1990**, *29*, 7133–7155.
- (7) Wallin, E.; von Heijne, G. *Protein Sci.* **1998**, *7*, 1029–1038.
- (8) Sansom, M. S. P. *Prog. Biophys. Mol. Biol.* **1991**, *55*, 139–236.
- (9) Kerr, I. D.; Sankararamakrishnan, R.; Smart, O. S.; Sansom, M. S. P. *Biophys. J.* **1994**, *67*, 1501–1535.
- (10) Randa, H. S.; Forrest, L. R.; Voth, G. A.; Sansom, M. S. P. *Biophys. J.* **1999**, *77*, 2400–2410.
- (11) Examples of studies of unsolvated peptides and proteins include the following: Suckau, D.; Shi, Y.; Beu, S. C.; Senko, M. W.; Quinn, J. P.; Wampler, F. M.; McLafferty, F. W. *Proc. Natl. Acad. Sci. U.S.A.* **1993**, *90*, 790–793. Campbell, S.; Rodgers, M. T.; Marzluff, E. M.; Beauchamp, J. L. *J. Am. Chem. Soc.* **1995**, *117*, 12840–12854. Schnier, P. D.; Price, W. D.; Jockusch, R. A.; Williams, E. R. *J. Am. Chem. Soc.* **1996**, *118*, 7178–7189. Kaltashov, I. A.; Fenselau, C. *Proteins: Struct. Funct. Genet.* **1997**, *27*, 165–170. Valentine, S. J.; Clemmer, D. E. *J. Am. Chem. Soc.* **1997**, *119*, 3558–3566. Wyttenbach, T.; Bushnell, J. E.; Bowers, M. T. *J. Am. Chem. Soc.* **1998**, *120*, 5098–5103. Artega, G. A.; Velázquez, I.; Reimann, C. T.; Tapia, O. *Phys. Rev. E* **1999**, *59*, 5981–5986. Schaaff, T. G.; Stephenson, J. L.; McLuckey, S. L. *J. Am. Chem. Soc.* **1999**, *121*, 8907–8919. Ruotolo, B. T.; Verbeck, G. F.; Thomson, L. M.; Gillig, K. J.; Russell, D. H. *J. Am. Chem. Soc.* **2002**, *124*, 4214–4215.
- (12) For a recent review, see: Jarrold, M. F. *Annu. Rev. Phys.* **2000**, *51*, 179–207.
- (13) Fenn, J. B.; Mann, M.; Meng, C. K.; Wong, S. F.; Whitehouse, C. M. *Science* **1989**, *246*, 64–71.
- (14) Light-Wahl, K. J.; Schwartz, B. L.; Smith, R. D. *J. Am. Chem. Soc.* **1994**, *116*, 5271–5278.
- (15) Loo, J. *Int. J. Mass Spectrom.* **2000**, *200*, 175–186.
- (16) Smith, R. D. *Int. J. Mass Spectrom.* **2000**, *200*, 509–544.
- (17) Counterman, A. E.; Valentine, S. J.; Srebalus, C. A.; Henderson, S. C.; Hoagland, C. S.; Clemmer, D. E. *J. Am. Soc. Mass Spectrom.* **1998**, *9*, 746–759.
- (18) Lee, S.-W.; Beauchamp, J. L. *J. Am. Soc. Mass Spectrom.* **1999**, *10*, 347–351.
- (19) Hudgins, R. R.; Jarrold, M. F. *J. Am. Chem. Soc.* **1999**, *121*, 3494–3501.
- (20) Hagen, D. F. *Anal. Chem.* **1979**, *51*, 870–874.
- (21) Von Helden, G.; Hsu, M.-T.; Kemper, P. R.; Bowers, M. T. *J. Chem. Phys.* **1991**, *95*, 3835–3837.
- (22) Clemmer, D. E.; Jarrold, M. F. *J. Mass Spectrom.* **1997**, *32*, 577–592.
- (23) Hudgins, R. R.; Ratner, M. A.; Jarrold, M. F. *J. Am. Chem. Soc.* **1998**, *120*, 12974–12975.
- (24) Hudgins, R. R.; Mao, Y.; Ratner, M. A.; Jarrold, M. F. *Biophys. J.* **1999**, *76*, 1591–1597.
- (25) Kinnear, B. S.; Jarrold, M. F. *J. Am. Chem. Soc.* **2001**, *123*, 7907–7908.
- (26) Kinnear, B. S.; Kaleta, D. T.; Kohtani, M.; Hudgins, R. R.; Jarrold, M. F. *J. Am. Chem. Soc.* **2000**, *122*, 9243–9256.
- (27) Kohtani, M.; Jarrold, M. F. *J. Am. Chem. Soc.* **2002**, *124*, 11148–11158.
- (28) Hudgins, R. R.; Dugourd, P.; Tenenbaum, J. M.; Jarrold, M. F. *Phys. Rev. Lett.* **1997**, *78*, 4213–4216.
- (29) Kinnear, B. S.; Hartings, M. R.; Jarrold, M. F. *J. Am. Chem. Soc.* **2001**, *123*, 5660–5667.
- (30) Gidden, J.; Bushnell, J. E.; Bowers, M. T. *J. Am. Chem. Soc.* **2001**, *123*, 5610–5611.
- (31) Wyttenbach, T.; Kemper, P. R.; Bowers, M. T. *Int. J. Mass Spectrom.* **2001**, *212*, 13–23.
- (32) Thölmann, D.; Tonner, S. C.; McMahon, T. B. *J. Phys. Chem.* **1994**, *98*, 2002–2004.
- (33) Dunbar, R. C.; McMahon, T. B.; Thölmann, D.; Tonner, S. C.; Salahub, D. R.; Wei, D. *J. Am. Chem. Soc.* **1995**, *117*, 12819–12825.
- (34) Price, W. D.; Schnier, P. D.; Williams, E. R. *Anal. Chem.* **1996**, *68*, 859–866.
- (35) Schnier, P. D.; Klassen, J. S.; Strittmatter, E. F.; Williams, E. R. *J. Am. Chem. Soc.* **1998**, *120*, 9605–9613.
- (36) Felitsyn, N.; Kitova, E. N.; Klassen, J. S. *Anal. Chem.* **2001**, *73*, 4647–4661.
- (37) Kitova, E. N.; Bundle, D. R.; Klassen, J. S. *J. Am. Chem. Soc.* **2002**, *124*, 5902–5913.
- (38) Kaleta, D. T.; Jarrold, M. F. *J. Am. Chem. Soc.* **2002**, *124*, 1154–1155.
- (39) Kaleta, D. T.; Jarrold, M. F. *J. Phys. Chem. A* **2002**, *106*, 9655–9664.
- (40) Mason, E. A.; McDaniel, E. W. *Transport Properties of Ions in Gases*; Wiley: New York, 1988.
- (41) Glasstone, S.; Laidler, K. J.; Eyring, H. *The Theory of Rate Processes*; McGraw-Hill: New York, 1941.
- (42) Benson, S. W. *Thermochemical Kinetics*, 2nd ed.; Wiley: New York, 1976.